Sipos, T., and Merkel, J. R. (1970), *Biochemistry 9,* 2766.
Smith, R. L., and Shaw, E. (1969), *J. Biol. Chem. 244,* 4704.
Solomon, I. (1955), *Phys. Rev. 99,* 559.
Stroud, R. M., Kay, L. M., and Dickerson, R. E. (1971), *Cold Springs Harbor Symp. Quant. Biol. 36,* 125.
Stroud, R. M., Kay, L. M., and Dickerson, R. E. (1974), *J. Mol. Biol. 83,* 185.
Titani, K., Ericsson, L. H., Neurath, H., and Walsh, K. A. (1975), *Biochemistry 14,* 1358.
Trowbridge, C. G., Krehbiel, A., and Laskowski, M. (1963), *Biochemistry 2,* 843.
Valenzuela, P., and Bender, M. L. (1969), *Proc. Natl. Acad. Sci. U.S.A. 63,* 1214.
Valenzuela, P., and Bender, M. L. (1970), *Biochemistry 9,* 2440.
Van Geet, A. L., and Hume, D. N. (1965), *Anal. Chem. 37,* 979.
Villanueva, G. B., and Herskovits, T. T. (1971), *Biochemistry 10,* 4589.
Walsh, K., and Neurath, H. (1964), *Proc. Natl. Acad. Sci. U.S.A. 52,* 884.
Yguerabide, J., Epstein, H. F., and Stryer, L. (1970), *J. Mol. Biol. 51,* 573.

The Molecular Structure of a Dimer Composed of the Variable Portions of the Bence-Jones Protein REI Refined at 2.0-Å Resolution†

Otto Epp,* Eaton E. Lattman,‡ Marianne Schiffer,§ Robert Huber, and Walter Palm#

ABSTRACT: The structure of the variable portions of a κ-type Bence-Jones protein REI forming a dimer has been determined by X-ray diffraction to a resolution of 2.0 Å. The structure has been refined using a constrained crystallographic refinement procedure. The final R value is 0.24 for 15,000 significantly measured reflections; the estimated standard deviation of atomic positions is 0.09 Å. A more objective assessment of the error in the atomic positions is possible by comparing the two independently refined monomers. The mean deviation of main-chain atoms of the two chains in internal segments is 0.22 Å, of main-chain dihedral angles 6.3° for these segments. The unrefined molecular structure of the V_{REI} dimer has been published (Epp, O., Colman, P., Fehlhammer, H., Bode, W., Schiffer, M., Huber, R., and Palm, W. (1974), *Eur. J. Biochem. 45,* 513). Now a detailed analysis is presented in terms of hydrogen bonds and conformational angles. Secondary structural elements (antiparallel β structure, reverse turns) are defined. A more precise atomic arrangement of the amino acid residues forming the contact region and the hapten binding site is given as well as the localization of solvent molecules. Two *cis*-prolines (Pro-8 and Pro-95) were detected. The intrachain disulfide bridge (Cys-23–Cys-88) occurs statistically in two alternative conformations. The structure suggests reasons for strong conservation of several amino acid residues. The knowledge of the refined molecular structure enables crystal structure analyses of related molecules to be made by Patterson search techniques. The calculated phases based on the refined structure are much improved compared to isomorphous phases. Therefore the effects of hapten binding on the molecular structure can be analyzed by the difference Fourier technique with more reliability. Hapten binding studies have been started.

Immunoglobulins are proteins with specific antibody activity. There exist several classes. The IgG class of immunoglobulins is composed of two light and two heavy chains. The Bence-Jones proteins excreted by patients with multiple myeloma into the urine have been shown to be free light chains. The Bence-Jones protein REI is a human immunoglobulin light chain of κ type. The purification, crystallization, and sequence analysis has been described (Palm, 1970; Palm and Hilschmann, 1973, 1975; Palm, 1974). The crystal structure of a dimer composed of the variable portions of this Bence-Jones protein at a resolution of 2.8 Å was reported (Epp et al., 1974). Data to a resolution of 2.0 Å have now been collected and the structure has been refined by constrained crystallographic refinement. The aim was to get a detailed insight into the conformation of this molecule (main chain, side chains, and bound solvent) and to obtain a model sufficiently accurate for its use in Patterson search techniques to determine the crystal structures of related molecules (Fehlhammer et al., 1975). As refined phases are considerably better than isomorphous phases (Watenpaugh et al., 1973; Deisenhofer and Steigemann, 1975; Huber et al., 1974), the quality of difference Fourier maps will be much improved; this will make it possible to determine the structure bound haptens and the subtle structural changes which might occur upon binding.

† From the Max-Planck-Institut für Biochemie, 8033 Martinsried bei München, West Germany, and Physikalisch-Chemisches Institut der Technischen Universität, München. *Received May 30, 1975.* The financial assistance of the Deutsche Forschungsgemeinschaft and Sonderforschungsbereich 51 is gratefully acknowledged.

‡ Present address: Rosenstiel Institute, Brandeis University, Waltham, Massachusetts 02154.

§ Was on leave from: Division of Biological and Medical Research, Argonne National Laboratory, Argonne, Illinois 60439.

Present address: Institut für Medizinische Biochemie der Universität Graz, Austria.

Table I: Options and Specifications of Various Programs.

(1) Model Building (Diamond, 1966)

Probe	Probe Length		Filter Constants C_1		Filter Constants C_2		Variation of Dihedral Angles
1	1	0[a]	0.5	1.0[a]	10^{-4}	10^{-2}[a]	ϕ,ψ,χ
2	1	2	0.5	0.5	10^{-4}	10^{-4}	ϕ,ψ,χ,τ
3	2	5	0.1	0.1	10^{-4}	10^{-4}	ϕ,ψ,χ,τ
4	5	6	0.1	0.0	10^{-4}	10^{-2}	ϕ,ψ,χ,τ
5	6	6	0.0	0.0	10^{-4}	10^{-2}	ϕ,ψ,χ,τ

Eigenshifts are permitted if either $\lambda \geq C_1\epsilon^2$ or $\lambda \geq C_2\lambda_{max}$, where λ are eigenvalues of the normal matrix. ϵ^2 is the residual. Variation of the folds of prolines, χ^5 of arginine, and ω was not permitted. The angular value of τ (N–C_α–C) was fixed to a value of 109.65° including model-building procedure 7. In model-building 7 *cis*-prolines were introduced (Huber and Steigemann, 1974). ϕ,ψ are main-chain dihedral angles, χ are side-chain dihedral angles. The angular values of main chain and side chains were used and included wherever they were known, even if only crudely.

(2) Real-Space Refinement (Diamond, 1971, 1974)

Zone length	7
Margin width	6; 8[b]
Fixed radius of all atoms (Å)	1.55; 1.50[c]
Relative weights of C:N:O:S	6:7:8:16
Relative softness of dihedral angles	
$\psi,\phi,\chi^1-\chi^4$	100
χ^5	1
$\theta^1,\theta^2,\theta^3$ (proline)	0.1
θ^1,θ^2 (cysteine)	0
τ (N–C_α–C)	0.1
ω (torsion angle $C_{i-1}{}^\alpha$–C_{i-1}–N_i–$C_i{}^\alpha$)	0.1[d]
Refinement of Scale Factor (K) and Background Level (d) Only	
Filter ratio $\lambda_{min}/\lambda_{max}$ for K, d refinement	0.01
Filter ratio for rotational refinement $\lambda_{min}/\lambda_{max}$	
Isomorphous map	0.005
from difference Fourier map 2 on	0.0005
from difference Fourier map 4 on	0.00007
from difference Fourier map 6 on	0.00004
The value of 0.00004 resulted in a proportion of shifts applied of about	70%
Filter ratio for translational refinement $\lambda_{min}/\lambda_{max}$	0.01
The value of 0.01 resulted in a proportion of shifts applied of about	100%

(3) Structure–Factor Calculation

(W. Steigemann and T. A. Jones) atomic scattering factors: Forsyth and Wells constants (1959), an overall temperature factor was used throughout.

(4) R Value Calculation

R is defined as $\dfrac{\Sigma\|F_o| - |F_c\|}{\Sigma|F_o|}$

$|F_o|$, observed structure–factor amplitude

$|F_c|$, calculated structure–factor amplitude

For this calculation, as well as for the Fourier calculations, reflections of extremely bad correlation were excluded. The condition for exclusion was:

$$\frac{2\|F_o| - |F_c\|}{|F_o| + |F_c|} > 1.2$$

About 250 reflections were excluded. The innermost reflections to 6.8-Å resolution were omitted from all calculations (941).

(5) Fourier Synthesis

Grid: 1.1 Å × 1.1 Å × 1.0 Å at the beginning to a resolution of 2.4 Å, later 0.8 Å × 0.8 Å × 0.8 Å. During the course of the refinement the Fourier coefficients were mostly of the type $(2|F_o| - |F_c|)\exp\alpha_c$. Also some Fourier syntheses with coefficients $(3|F_o| - 2|F_c|)\exp\alpha_c$ were used. Difference Fourier maps were calculated with coefficients $(|F_o| - |F_c|)\exp\alpha_c \cdot \alpha_c$, calculated phase.

(6) Computer Time on a Siemens 4004/150 (Cycle Time 0.75 μsec)

Structure–factor calculation for 15,000 reflections and 1630 atoms	13,500 sec
Fourier synthesis 1.62×10^5 grid points	4000 sec
Real-space refinement for both chains in the asymmetric unit	17,000 sec

[a] These values were used in model-building procedures 8 and 9 for probe length and filter constants. Also the variation of the angular value of τ was allowed, but not for Gly, Ser, and Thr. [b] After introduction of ω. [c] New value estimated with the data at 2.1-Å resolution. [d] ω has been introduced after difference Fourier map 4 (data to 2.3-Å resolution, R factor value 0.29, B = 23 Å^2).

Experimental Procedure

The V_{REI} dimer crystallizes in the space group $P6_1$. The hexagonal unit cell parameters are $a = b = 75.8$ Å, $c = 98.2$ Å, $\gamma = 120°$. The asymmetric unit contains one dimer molecule. Intensity data were collected to 2.0-Å resolution on a modified Siemens AED diffractometer using θ–2θ scan, with focus-to-crystal and crystal-to-detector distances of 30 cm each. The intensity profile of each reflection was scanned twice in steps of 1/100° (44 steps over the whole reflection). The counting time per step was set inversely proportional to the intensity at the peak of the reflection; the upper limit was set at 2.4 sec/step for reflections to a resolution of 2.5 Å. The reflections from 2.5- to 2.0-Å resolution were measured with 6 sec/step. Background was counted on both sides. The whole data set had been collected by diffractometers. The reflections were collected in shells of sin θ/λ. Film data obtained from screenless precession photographs which were evaluated using the method of Schwager et al. (Schwager et al., 1975) were included and used for scaling purposes. The data were corrected for absorption by an empirical method (Huber and Kopfmann, 1969). The complete intensity data set included 42,464 measurements (of which 5454 are film data), which were merged to 14,993 independent reflections (0.69 of the possible reflections to a resolution of 2.0 Å). All reflections to a resolution of 2.5 Å were used (10381), except the innermost reflections to a resolution of 6.8 Å (941) which are strongly influenced by the solvent continuum. To a resolution of 2.5 Å, 0.99 of the possible reflections is measured. From 2.5- to 2.0-Å resolution, only the reflections which could be observed above the 2σ significance level determined from counting statistics (3671) were used (e.g., 0.34 of the possible reflections in that range).

The neglect of the innermost reflections to a resolution of 6.8 Å does not influence Diamond's real-space refinement procedure. In the refinement of PTI (Deisenhofer and

Steigemann, 1975) the neglect of the innermost reflections improved the refinement of the positions of solvent molecules. We omitted these reflections from all calculations and did not consider them in the interpretation of the electron density map. The R value for all measurements, defined as

$$R = \left(\sum_h \sum_j^{N_h} (\langle I \rangle_h - I_{hj})^2 \Big/ \sum_h N_h \langle I \rangle_h^2 \right)^{1/2}$$

is 0.05 ($\langle I \rangle_h$ is the average intensity of the N_h measurements, I_{hj} are the individual measurements of a reflection h). The R_{sym} values for individual crystals lie between 0.022 and 0.065; the average R_{sym} is 0.04.

The crystal structure of REI has been refined by a constrained crystallographic refinement described in the refinement of the crystal structure of the bovine pancreatic trypsin inhibitor (PTI) (Deisenhofer and Steigemann, 1975) and in the refinement of the structure of the complex between bovine trypsin and PTI (Huber et al., 1974). This procedure involves cycles consisting of phase calculation using the current atomic model, Fourier synthesis using these calculated phases and the observed structure-factor amplitudes, and Diamond's real-space refinement (Diamond, 1971, 1974). At various stages (stagnation of further refinement), difference Fourier syntheses are calculated to detect and correct gross errors in the model (such as incorrect orientation of main-chain amides or side chains) and to localize solvent molecules. The stagnation of the refinement is reached, if the R factor value (definition see Table I) does not decrease further. Incorrectly oriented main-chain amides are rotated by reading the correct position of the carbonyl oxygen from the difference map and subjecting the whole chain to a model-building procedure (Diamond, 1966). Side-chain orientations are corrected by rotating around the appropriate dihedral angles. Some characteristics of the model-building procedure and the real-space refinement procedure are outlined in Table I. During the refinement 8 model-building procedures and 11 difference Fourier syntheses were calculated. The Fourier syntheses in the automatic cycles between these difference Fourier maps were mostly of the type $(2|F_o| - |F_c|) \exp \alpha_c$; a few $(3|F_o| - 2|F_c|) \exp \alpha_c$ were also used. Such syntheses increase the density gradients at the atomic positions and the speed of convergence. Table II shows the statistics of the course of the real-space refinement procedure.

Table II: Specifications of Difference Fourier Maps.

Difference Map No.	R Value	Corrections in Each Map: Side Chains Main-Chain Amides Chain 1	Chain 2	Resolution (Å)	Overall Temp Fact. (Å²)	Atom Radius ⟨r⟩(Å)
1	0.390	10	7	2.5	28	1.55
2	0.350	4	6	2.4	25	1.55
3	0.304	3	2	2.4	23	1.55
		11 solvent molecules				
4	0.294	4	2	2.3	23	1.55
		26 solvent molecules				
5	0.282	4	3	2.3	23	1.55
		40 solvent molecules				
6	0.270	1	1	2.2	23	1.55
		39 solvent molecules introduction of cis-prolines (Pro-8, Pro-95)				
7	0.264	1	1	2.2	23	1.55
		42 solvent molecules				
8	0.250	1	1	2.2	23	1.55
		36 solvent molecules				
9	0.241			2.1	23	1.55
		41 solvent molecules				
10	0.241			2.1	23	1.50
		55 solvent molecules				
11	0.241			2.0	21	1.50
		53 solvent molecules				

Results and Discussion

Description of the Refinement. The starting model had been obtained through extensive real-space refinement of the model into the isomorphous Fourier map at 2.8-Å resolution. The above electron density map had first been averaged over the two independent molecules (Epp et al., 1974). The starting R factor (defined in Table I, 4) was 0.48. During the subsequent course of the refinement the two molecules in the asymmetric unit were refined independently. The coordinates of the second molecule were obtained by applying the known local symmetry. After several cycles the R factor decreased to a value of 0.39. At this stage, the first difference Fourier map was calculated. The coordinates were plotted onto the Fourier map to check the progress. Misplaced side chains and several incorrectly oriented main-chain amides were detected (Table II). Between succeeding difference Fourier maps three to five automatic refinement cycles were performed, depending on the progress of the refinement. The refinement was started with reflection data to 2.5-Å resolution. During the course of the refinement further data were included to 2.0-Å resolution. An overall temperature factor was used, which was recalculated several times by comparing $|F_o|$ and $|F_c|$ and the temperature factor changed if necessary. An average atomic radius of 1.55 Å was used for all atoms throughout the refinement until difference Fourier map 9. Afterwards a new value of 1.50 Å was estimated by a trial calculation of atomic radii refinement in the real-space refinement step. This value is directly related to and consistent with the observed overall temperature factor of 21 Å². By the inspection of the difference Fourier maps, solvent molecules were detected and used in the phase calculations. The course of the difference maps is shown in Table II. The starting model had to be corrected in several segments. A number of main-chain amides and side chains had to be rotated. For the correction of main-chain amides, the presence of two identical molecules in the asymmetric unit provided a very useful cross-check. In difference Fourier map 6, the segments around Pro-8 and Pro-95 could be corrected. The local distribution of maxima and minima in these two regions was very similar and consistent in the two independent molecules, and it suggested the presence of cis-peptide groups (Huber and Steigemann, 1974). After the introduction of these *cis*-prolines, the refinement proceeded and stopped finally at an R factor value of 0.24. At this stage, 53 solvent molecules had been identified.

Description of the Electron Density Map. Figure 1a and b is stereo pictures of the electron density and the model fit at two amino acid residues (Gln-37 and Tyr-71)[1] in order to

[1] Amino acid residue numbers are those of the V_{REI} sequence. The nomenclature recommended by IUPAC-IUB (1970) is used in this paper with additional definitions as given by Diamond (1966, 1971, 1974). The coordinates of the V_{REI} dimer are available upon request. They are also in the Protein Data Bank of Brookhaven National Laboratory. Coordinates as well as stereo drawings are contained in R. Feldmann's Global Atlas of Protein Structure on Microfiche.

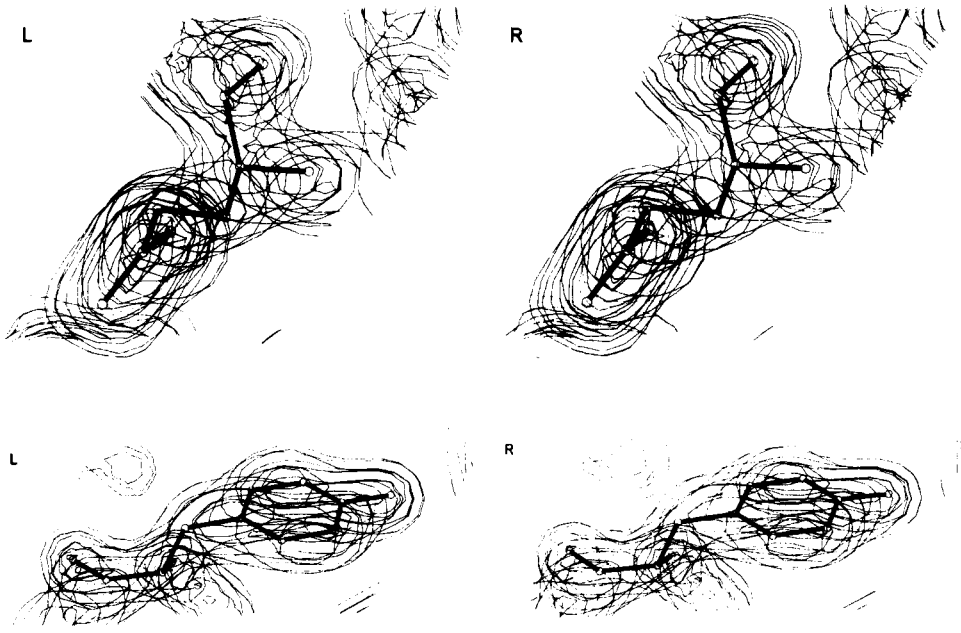

FIGURE 1: Electron density and model fit at two amino acid residues (top, Gln-37; bottom, Tyr-71). Contours in these figures from 0.3 e/Å^3 in steps of 0.3 e/Å^3.

demonstrate the quality of the final Fourier map. A typical electron density for carbon is 0.8 e/Å^3 and for oxygen 0.9 e/Å^3.

The final difference Fourier map is clear and suggests that the molecular structure is correctly interpreted. There is still some positive and negative residual density. Because of the restricted rotations about the S–S bond, cystine can exist in two mirror-image forms (Beychok, 1967). In the V_{REI}[2] monomer there is one intrachain disulfide bridge (Cys-23–Cys-88). Both conformations, differing predominantly in the position of 23 S^{γ}, occur statistically in about the same proportion in each monomer. This is shown in Figure 2a and b where sections 27–34 of difference Fourier maps ($F_o - F_c$) based on both conformations are drawn for monomer 2. Figure 2a shows the final difference map.

Figure 2b shows a difference map based on the alternative cystine conformation in the molecule. The difference between the two configurations is essentially expressed in the value of the side-chain dihedral angle χ^3 (rotation about the S–S bond). It differs by 162°. The final difference Fourier map also shows two statistical positions for the side chain of Gln-100.

Besides these there are about 40 negative peaks with height −0.20 e/Å^3, 20 with height −0.25 e/Å^3, and a few with height −0.30 e/Å^3. About 15 residual density peaks are positive, the highest is +0.25 e/Å^3. The positive peaks are near atomic positions, the negative features occur mainly at carbonyl oxygens, at the badly defined region of the N-terminus, at Gly-41, and at C^{ϵ} and N^{ζ} of lysine side chains. The negative residual density at carbonyl oxygens has also been observed in the PTI–trypsin complex and suggests that main-chain vibration affects predominantly the carbonyl oxygens. Six of the 53 water molecules found at the end of the refinement, and included in the calculations with full occupancy and a temperature factor of 21 Å^2, lie in negative density of −0.25 e/Å^3.

Accuracy of the Structure; Comparison of the Two Monomers. A comparison of the dihedral angles of the two main chains shows that only at the N- and C-termini, which are badly defined, at some Gly residues (Gly-57, Gly-64), and in some external loops (12–18, 26–34 first hypervariable region, 40–44, 78–81, 93–97 part of the third hypervariable region) the differences between the two chains are considerably larger than the mean deviation $\langle \Delta\phi,\psi \rangle$ of 9.6°. There are particularly large discrepancies in ϕ and ψ at Ser-26, Gln-27, and Asp-28. We observed no significant deviation in dihedral angles of residues forming the monomer–monomer contact across the local diad (see Figure 5). The segments deviating significantly from the local symmetry face the solvent, and the reasons for these structural differences are unclear. As the difference map is featureless in these regions (Gln-27 is visible only to C^{γ} in both chains) these structures appear to represent real alternative conformations. The mean deviation excluding these segments is $\langle \Delta\phi,\psi \rangle$: 6.3°. The same result is reflected by a comparison of the main-chain atoms (N, C^{α}, C^{β}, C, O) of internal segments of both monomers (segments 4–10, 19–25, 35–38, 45–49, 62–77, 84–89, and 97–102). The mean deviation $\langle r \rangle$ is 0.22 Å compared with 0.47 Å for all atoms (the mean deviation of the internal segments for PTI and PTI complexed with trypsin is 0.25 Å, Huber et al., 1974). The average shift of main-chain atoms from the starting model (identical monomers) to the final model was 0.79 Å neglecting N- and C-terminal segments. A comparison of side-chain dihedral angles shows larger differences, especially at residues Ser, Thr, Gln, and Lys.

An objective assessment of the error of 0.2 Å, in the atomic coordinates of the final model, is possible by comparing the two chains forming the dimer. This estimate is an upper limit because there may be small structural alter-

[2] Abbreviations used are: $F_{ab'}$, antigen-binding fragment of immunoglobulins; V_{REI}, variable part of the Bence-Jones protein REI; V_L, variable part of light chain; L1, L2, and L3 are the first, second, and third hypervariable regions of light chains; κ, λ, the two major types of light chains differentiated by their C-terminal amino acid sequences; Dnp, 2,4-dinitrophenyl.

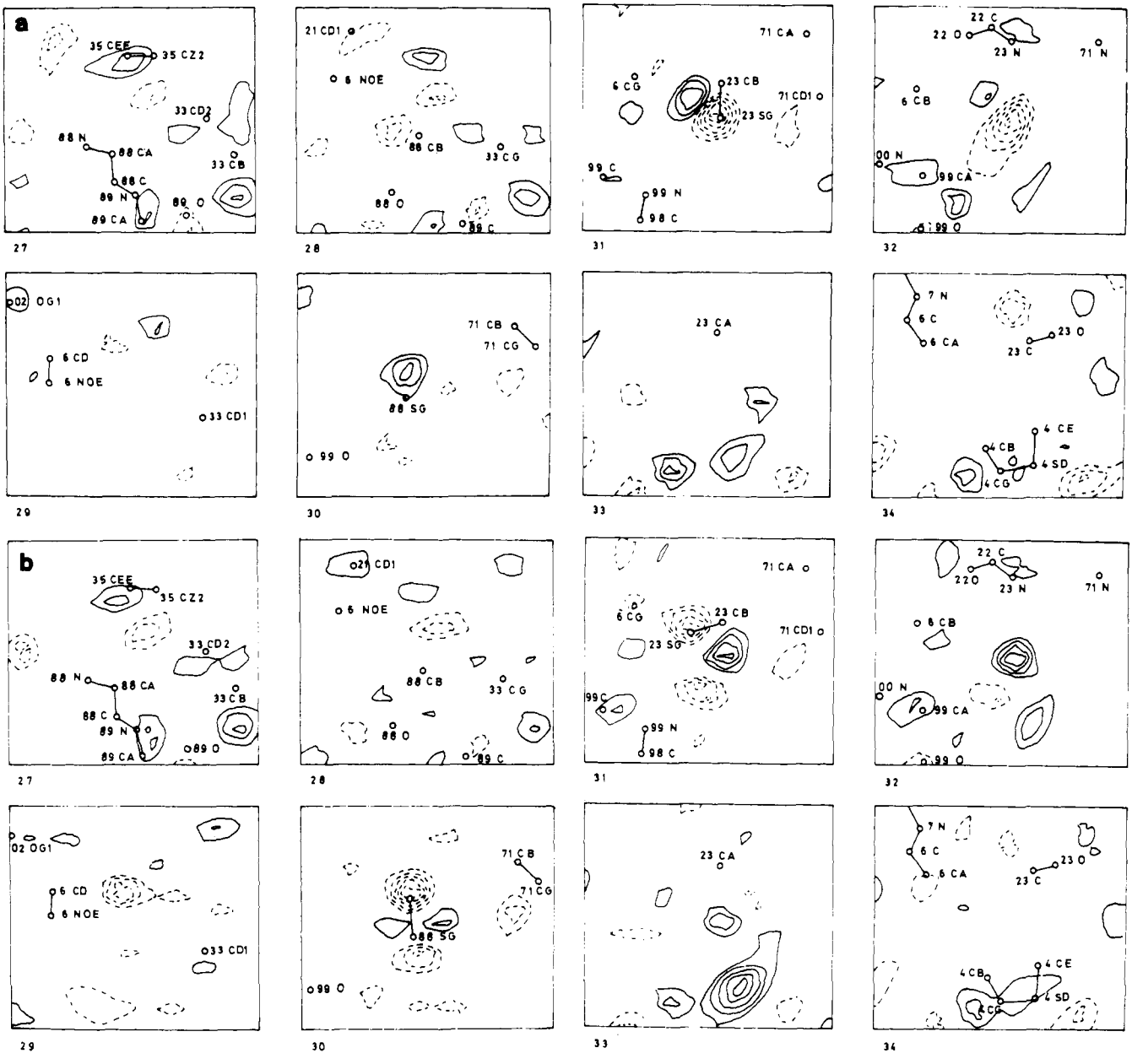

FIGURE 2: Sections 27–34 of difference Fourier maps ($F_o - F_c$) based on one of both possible cystine (Cys-23–Cys-88) conformations, respectively (shown is monomer 2). Contours from 0.10 e/Å^3 in steps of 0.05 e/Å^3: (—) positive, (- - -) negative residual densities. (a) Final difference map; (b) an intermediate state of the refinement. This explains the high residual density below Met-4 SD.

ations on dimer formation.

An estimate of the accuracy of the final atomic positions can also be deduced by Cruickshank's formulas using the residual and the curvature of the electron density at the atomic positions (Cruickshank, 1949). The mean height of carbonyl oxygens in the final Fourier map is 0.9 e/Å^3. This yields a curvature of −1.32 e/Å^5 (Stout and Jensen, 1968; Watenpaugh et al., 1973). The resulting standard deviation is $\sigma(x)$ = 0.09 Å. This is comparable to the values obtained for PTI-trypsin complex (Huber et al., 1974).

Description of the Monomer. The V_{REI} monomer has a sandwich-like structure. The polypeptide chain can be divided into nine segments, which form two halves partly consisting of anti-parallel β structure. These segments are connected by reverse turns. The two sheets cover a hydrophobic interior containing several invariant or almost completely conserved amino acid residues in κ-light chains (Epp et al., 1974). The upper part consists of five strands, the bottom part of three strands. The N-terminal strand adds to the upper sheet in a parallel and to the lower sheet in an anti-parallel fashion. The lower part is a rather regular anti-parallel β-pleated sheet. An analysis of the conformational angles of the participating amino acid residues (5–7, 19–24, 63–65, and 71–75) yields mean values for ϕ and ψ of −117 and +140°, respectively, with standard deviations of 15 and 16°.

The ϕ and ψ values for a regular anti-parallel β structure (β-poly(L-alanine)) are −139 and +135° (Arnott et al., 1967). The remaining residues of the lower molecular part are involved in reverse turns. In the upper part, a regular antiparallel β-structure conformation is formed by two strands containing the residues 34–38 and 85–89. The analysis of the conformational angles yields mean values for ϕ and ψ of −116 and +137° with standard deviations of 13 and 11°, respectively. The other three strands of that molecular part are attached in a more irregular β structure.

Table III: Intramolecular Hydrogen Bonds.

Main Chain		Main Chain		Chain 1 Chain 2 d (Å)	d (Å)	$\langle d \rangle$ (Å)
Thr-5	NH	Gln-24	C=O	2.9	3.1	3.0
Thr-5	C=O	Gln-24	NH	2.9	3.0	3.0
Ser-7	NH	Thr-22	C=O	3.1	3.0	3.1
Ser-7	C=O	Thr-22	NH	2.7	2.8	2.8
Leu-11	NH	Lys-103	C=O	3.1	3.0	3.1
Leu-11	C=O	Gln-105	NH	3.0	3.0	3.0
Ala-13	C=O	Thr-107	NH	2.5		
Ser-14	C=O	Asp-17	NH	3.0	3.1	3.0
Gln-16	NH	Leu-78	C=O	2.9	2.9	2.9
Ser-17	C=O	Leu-78	NH		3.2	
Val-19	C=O	Ile-75	NH	3.1	3.0	3.0
Val-19	NH	Ile-75	C=O		3.1	
Ile-21	NH	Phe-73	C=O	3.0	3.0	3.0
Ile-21	C=O	Phe-73	NH	2.9	2.8	2.9
Cys-23	NH	Tyr-71	C=O	2.9	2.9	2.9
Cys-23	C=O	Tyr-71	NH	2.9	2.8	2.9
Ala-25	NH	Thr-69	C=O	2.8	2.9	2.8
Ile-29	C=O	Tyr-32	NH	3.0	2.9	2.9
Ile-29	NH	Gly-68	C=O		3.1	
Ile-30	C=O	Gly-68	NH	3.2		
Leu-33	C=O	Ala-51	NH	2.8	2.7	2.7
Asn-34	NH	Gln-89	C=O	2.8	2.9	2.8
Asn-34	C=O	Gln-89	NH	2.9	2.9	2.9
Trp-35	NH	Ile-48	C=O	3.0	2.9	3.0
Trp-35	C=O	Leu-47	NH	3.0	2.8	2.9
Tyr-36	NH	Tyr-87	C=O	2.6	2.6	2.6
Tyr-36	C=O	Tyr-87	NH	2.9	2.8	2.8
Gln-37	NH	Lys-45	C=O	2.9	2.9	2.9
Gln-37	C=O	Lys-45	NH	2.8	2.8	2.8
Gln-38	NH	Thr-85	C=O	2.9	2.7	2.8
Gln-38	C=O	Thr-85	NH	2.9	3.1	3.0
Thr-39	C=O	Lys-42	NH		3.2	
Tyr-49	NH	Asn-53	C=O	3.0	3.0	3.0
Tyr-49	C=O	Asn-53	NH	3.0	2.9	3.0
Arg-61	C=O	Ser-76	NH	2.8	2.9	2.9
Ser-63	C=O	Thr-74	NH	3.1	2.9	3.0
Ser-63	NH	Thr-74	C=O		2.9	
Ser-65	NH	Thr-72	C=O	3.1	3.2	3.1
Ser-65	C=O	Thr-72	NH	2.8	3.0	2.9
Ala-84	C=O	Leu-104	NH	3.0	3.1	3.1
Tyr-86	NH	Thr-102	C=O	2.9	3.0	3.0
Tyr-86	C=O	Thr-102	NH	2.9	3.1	3.0
Cys-88	C=O	Gly-99	NH	2.8	2.8	2.8

Main Chain		Side Chain		Chain 1 Chain 2 d (Å)	d (Å)	$\langle d \rangle$ (Å)
Ile-2	C=O	Thr-97	OH	2.9	2.7	2.8
Pro-8	C=O	Thr-102	OH	2.8	2.7	2.7
Ser-14	NH	Asp-17	COO^-	2.8	3.0	2.9
Ala-25	C=O	Thr-69	OH		2.6	
Ile-30	NH	Asp-28	COO^-	2.8		
Gln-79	NH	Asp-82	COO^-	3.1		
Asp-82	C=O	Tyr-86	OH	2.7	2.8	2.8
Tyr-86	C=O	Gln-6	$O=C-NH_2$	2.7	2.7	2.7
Gln-92	NH	Gln-90	$O=C-NH_2$	2.9	2.7	2.8
Pro-95	C=O	Gln-90	$O=C-NH_2$	3.0	3.1	3.1

Side Chain		Side Chain		Chain 1 Chain 2 d (Å)	d (Å)	$\langle d \rangle$ (Å)
Gln-6	$O=C-NH_2$	Thr-102	OH	2.9	2.9	2.9
Asn-34	$O=C-NH_2$	Gln-89	$O=C-NH_2$		3.1	
Tyr-36	OH	Gln-89	$O=C-NH_2$	3.0	3.0	3.0
Arg-61	NH_2	Asp-82	COO^-	2.7	2.9	2.8
Arg-61	NH_2	Gln-79	$O=C-NH_2$		2.7	

One strand is the carboxyl-terminal end, another the segment containing the residues 43-50, which makes a kink, possibly to allow all three consecutive hydrophobic residues (Leu-46, Leu-47, and Ile-48) to lie in the interior of the molecule. The third strand is the segment from amino acid residues 51-61, which forms a large loop containing two reverse turns. In this segment is a deletion of seven amino acid residues in the V_L part of the Fab′ fragment of a human myeloma immunoglobulin IgG1(λ) New (Poljak et al., 1974). Such a deletion must cause a considerable rearrangement of the peptide chain, possibly from Tyr-49 on. Leu-46 to Ile-48 is conserved in sequence and possibly also in position as well as Arg-61. The upper half contains two hypervariable regions L2 (amino acid residues 50-56) and L3 (89-97), whereas L1 (28-34) is an extended polypeptide chain connecting both sheets.

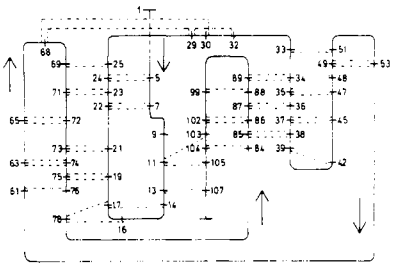

FIGURE 3: Hydrogen-bonding scheme of the main-chain atoms of a monomer of V_{REI}.

Table III lists the intramolecular hydrogen bonds of the two monomers (main-chain bonds, main-chain-side-chain bonds and side-chain bonds) and their donor-acceptor distances. A hydrogen bond was counted when the donor-acceptor distance was less than 3.2 Å and the angles were stereochemically reasonable. This is a more stringent condition than was applied previously, hence less hydrogen bonds were found. Figure 3 shows the hydrogen-bonding scheme of the main-chain atoms. Most of the hydrogen bonds postulated in our preliminary model have been confirmed (compare Figure 3 with Figure 3(B) in Epp et al., 1974). The hairpin bends (Venkatachalam, 1968; Crawford et al., 1973) could also be confirmed and a few further bends were characterized (Table IV). It became clear during the course of refinement that two out of six prolines (Pro-8 and Pro-95) of the molecule are *cis*-prolines (Huber and Steigemann, 1974). Both residues lie in the third position of reverse turns and are nearly conserved in κ-type light chains. The presence of these two X-Pro cis-peptide groups in κ-light chains and the observation of *cis*-Pro bends in several other protein molecules suggest that this is an important structural element.

Interdomain Contacts. The monomer-monomer contact can be classified into two parts, the contact region A and the hapten binding site B. The amino acid residues Tyr-36, Gln-38, Ala-43, Pro-44, Tyr-87, Gln-89, Phe-98, and two parts of the polypeptide chain (Lys-42, Gly-99) of both monomers participate in the contact region. The hydrophobic core formed of residues Tyr-36, Ala-43, Pro-44, Tyr-87, and Phe-98 encloses a small cavity and is terminated on the backside by hydrogen-bonded Gln-38 residues. In the front are the polar residues Gln-89 making hydrogen bonds to the phenolic groups of both Tyr-36 residues. The arrangement of these residues has a twofold symmetry within the limits of error; this symmetry is shown in Figure 5. Phe-98 is invariant in all light chains; the other residues are almost completely conserved.

The hapten binding site lies in front of the contact region along the local twofold axis. Residues Tyr-32, Tyr-36, Tyr-49, Tyr-91, Tyr-96, Asn-34, Gln-89, Leu-46, and Leu-94 from both monomers contribute to the hapten binding site forming a slit-like pocket. The spatial arrangement of these residues can be seen in Figure 6 viewed along the local diad.

Table IV: Hairpin Bends in Both Monomers.[a]

Segment	$C_1^\alpha \ldots C_4^\alpha$ Distance (Å)	$O_1 - N_4$ Distance (Å)	$\phi_2, \psi_2, \phi_3, \psi_3$[b] (deg)	Type
Ser[14]-Val[15]-Gly[16]-Asp[17]	5.9	3.0	−84, 151, 79, −19	RT II
	5.8	3.1	−69, 138, 97, −33	
Ile[29]-Ile[30]-Lys[31]-Tyr[32]	5.8	3.0	79, −78, −146, 21	NR II′
	5.7	2.9	72, −67, −165, 19	
Thr[39]-Pro[40]-Gly[41]-Lys[42]	5.9	>3.2	−68, 132, 67, 3	RT II
	5.6	3.2	−59, 120, 90, −16	
Gln[55]-Ala[56]-Gly[57]-Val[58]	6.1	>3.2	−61, 136, 67, 4	NR II
	6.0	>3.2	−76, 138, 92, −22	
Pro[59]-Ser[60]-Arg[61]-Phe[62]	6.2	>3.2	−91, −8, −57, −20	NR III
	6.0	>3.2	−83, −8, −63, −32	
Ser[67]-Gly[68]-Thr[69]-Asp[70]	6.4	>3.2	77, −111, −114, −20	O II′
	6.3	>3.2	77, −101, −121, −30	
Gln[79]-Pro[80]-Glu[81]-Asp[82]	5.5	3.2	−53, −30, −105, 14	RT I
	5.9	3.2	−59, −29, −82, 14	
Gln[6]-Ser[7]-Pro[8]-Ser[9][c]	6.7		−151, 147, −66, −177	O
	6.6		−136, 149, −60, −175	
Ser[93]-Leu[94]-Pro[95]-Tyr[96][c]	6.6		−88, 154, −62, 149	O
	6.6		−74, 148, −86, 169	

[a] Characterization according to the definitions suggested by Crawford et al. (1973). RT, reverse turn; NR, near reverse turn; O, open turn. [b] C_1^α, C_4^α α-carbon atoms of residues 1 and 4; O_1 carbonyl oxygen of residue 1; N_4 nitrogen of residue 4; $\phi_2, \psi_2, \phi_3, \psi_3$ main-chain dihedral angles of residues 2 and 3. [c] May be regarded as open turns (Huber and Steigemann, 1974).

Table V: Listing of Residues Which Form Contacts between the Monomers in the Range of 2.2–4.0 Å.[a]

Residues	Atoms	d (Å)	Atoms	d (Å)
		Contact Region		
Gln-38, Gln-38	Gln-38 NOE1	3.1 H	Gln-238 NOE2	
	Gln-38 NOE2	2.9 H	Gln-238 NOE1	
Tyr-36, Gln-89	Tyr-36 OEE, Gln-289 NOE2	3.2 H	Tyr-236 OEE, Gln-89 NOE2	3.8
Tyr-36, Phe-98	Tyr-36, CE2 Phe-298 CE1	3.4	Tyr-236 CE2, Phe-98 CE1	3.5
	Tyr-36 CE2, Phe-298 CZ	4.0		
			Tyr-236 CD2, Phe-98 CE1	3.9
Gln-38, Tyr-87			Gln-238 NOE2, Tyr-87 OEE	3.7
Lys-42, Tyr-87	Lys-42 C=O, Tyr-287 OEE	3.4	Lys-242 C=O, Tyr-87 OEE	3.5
Ala-43, Tyr-87	Ala-43 CA, Tyr-287 CE1	3.8	Ala-243 CA, Tyr-87 CE1	3.9
			Ala-243 CB, Tyr-87 CE1	3.9
Ala-43, Phe-98	Ala-43 CB, Phe-298 CB	3.8	Ala-243 CB, Phe-98 CB	3.8
Ala-43, Gly-99	Ala-43 CB, Gly-299 C=O	3.1	Ala-243 CB, Gly-99 C=O	3.3
Pro-44, Tyr-87	Pro-44 CD, Tyr-287 CZ	3.8		
	Pro-44 CD, Tyr-287 CE1	3.8		
Pro-44, Phe-98	Pro-44 CG, Phe-298 CD2	3.6		
	Pro-44 CG, Phe-298 CE2	3.7	Pro-244 CG, Phe-98 CE2	3.8
			Pro-244 CG, Phe-98 CZ	3.7
	Pro-44 CG, Phe-298 CD1	3.8	Pro-244 CG, Phe-98 CD1	3.9
	Pro-44 C=O, Phe-298 CD1	3.4	Pro-244 C=O, Phe-98 CD1	3.2
	Pro-44 C=O, Phe-298 CG	3.9	Pro-244 C=O, Phe-98 CG	3.9
			Pro-244 C=O, Phe-98 CE1	3.9
	Pro-44 C=O, Phe-298 CB	3.7		
			Pro-244 C, Phe-98 CD1	3.9
			Pro-244 CG, Phe-98 CE1	3.8
			Pro-244 CB, Phe-98 CE1	3.9
	Pro-44 CG, Phe-298 CG	3.7		
		Hapten Binding Site		
Leu-46, Tyr-96	Leu-46 CD2, Tyr-296 N	4.0	Leu-246 CD2, Tyr-96 N	3.6
			Leu-246 CD2, Tyr-96 CB	3.8
			Leu-246 CB, Tyr-96 C=O	3.7
Tyr-49, Leu-94	Tyr-49 CD1, Leu-294 CD2	3.7	Tyr-249 CD1, Leu-94 CD2	4.0
	Tyr-49 CG, Leu-294 CD2	3.9	Tyr-249 CG, Leu-94 CD2	3.8
			Tyr-249 CD1, Leu-94 CD1	3.8
			Tyr-249 CD2, Leu-94 CD2	3.8
			Tyr-249 CE1, Leu-94 CD1	3.8
	Tyr-49 CE1, Leu-294 CD2	3.8		
	Tyr-49 CE2, Leu-294 CD1	3.9		

[a] Subunit 2 has 200 added to amino acid numbers.

The bottom is made by the polar Gln-89 residues hydrogen-bonded to the phenolic groups of Tyr-36 residues (front of the contact region). The walls are formed by tyrosines-49, -91, -96, leucines-46, and the polar asparagines-34 near the bottom. At the mouth of the pocket the residues Tyr-32 and Leu-94 are situated. It is interesting to note that the Bence-

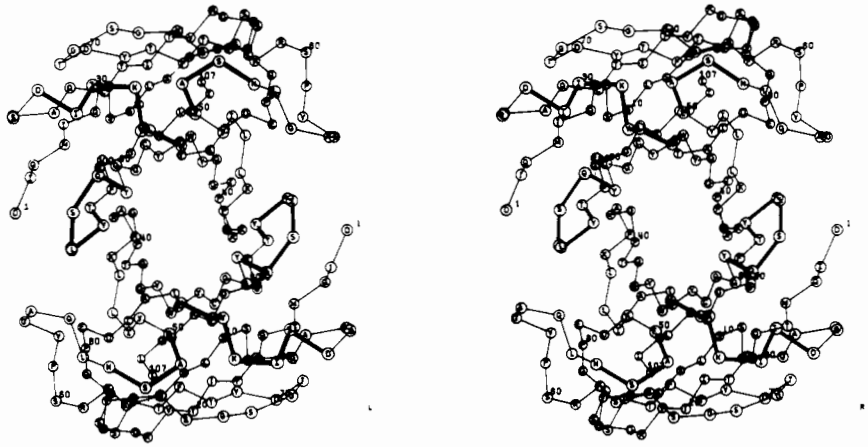

FIGURE 4: Stereo drawing of the α-carbon atoms of the V_{REI} dimer as seen along the local diad axis. The hypervariable segments are indicated by heavy lines; the amino acid residues are marked by the one letter code.

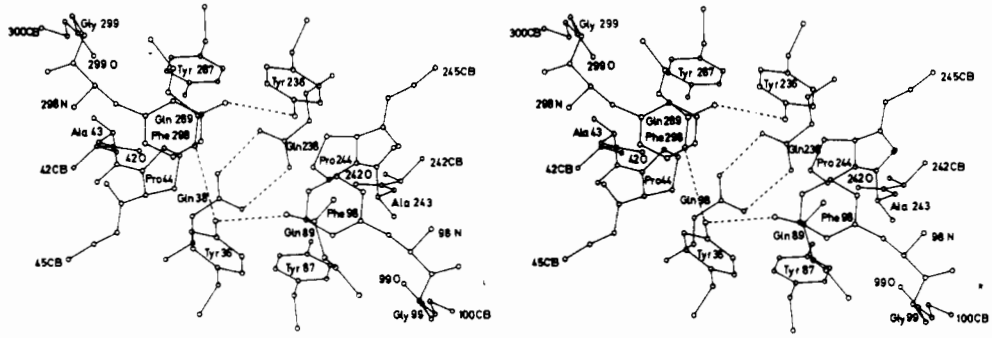

FIGURE 5: Stereo drawing of the residues forming the contact in the V_{REI} dimer as seen along the local diad.

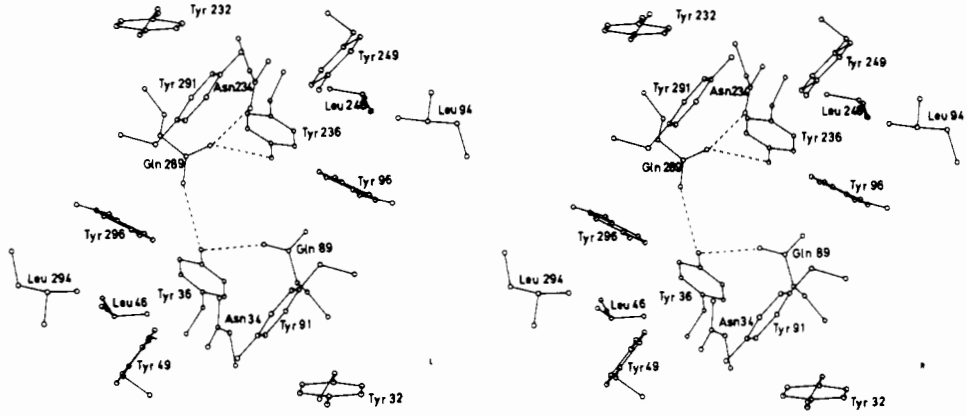

FIGURE 6: Stereo drawing of the residues forming the hapten-binding site of the V_{REI} dimer as seen along the local diad.

Jones protein AU, which differs in 16 amino acids from REI, has Tyr-96 substituted for a tryptophan. The structure analysis of V_{AU} (Fehlhammer et al., 1975) showed that the indole ring extends into the binding pocket, making it much smaller. A single amino acid substitution may drastically alter the hapten binding properties.

Table V lists the atomic distances in the range of 2.2–4.0 Å between amino acid residues participating in the contact region and the hapten binding site. Figures 4–6 are stereo drawings of the final atomic coordinates. Figure 4 is a stereo drawing of the α-carbon atoms in the dimer seen along the local diad axis; the hypervariable regions are indicated by heavy lines. Residues are marked by the one letter code. The main-chain atoms of the hypervariable regions form a large cavity, partly filled by the amino acid side chains forming the hapten binding site.

Position of Solvent Molecules. In the course of refinement, 53 solvent molecules were localized in the asymmetric unit. Water molecules were introduced at relative high electron density peaks occupying stereochemically reasonable positions. The atomic distances of the water molecules making hydrogen bonds to polar groups of the dimer are listed in Table VI (range 2.3–3.3 Å). The table lists solvent molecules linking intrachain polar groups of both monomers. One water molecule (numbered 429) makes an interchain hydrogen bond. A number of solvent molecules are hydrogen bonded to one polar group of monomer 1 or 2, respectively. Further water molecules are hydrogen bonded to

other water molecules (not included in Table VI, because the calculated distances are out of range). The positions of the water molecules are not as accurately determined as the atoms of the protein moiety. They are often broadened in the electron density map. The mean value of the height of these peaks in the final Fourier map is only 0.75 e/Å^3 compared to 0.90 e/A^3 to oxygen atoms, demonstrating incomplete occupation and higher mobility. Most solvent molecules lie at the surface of the dimer; only a few are internal. Two of the latter (numbered 406 and 420) occupy the same positions in both monomers; they are hydrogen-bonded to N$^\epsilon$ of Trp-35 and the carbonyl oxygen of Ala-51. About half of the solvent molecules on the surface of the dimer lie at similar positions in both monomers, the others are visible only at monomer 1 or 2 (see Table VI). Three water molecules, presumably hydrogen bonded to each other, are present in the small partially hydrophobic cavity found in the contact region (Figure 5). Although the enclosed water molecules are not associated with any single polar group, their presence in the cavity is certain by the difference Fourier map.

Binding experiments of 2,4-dinitrophenyl compounds and other small molecules to a crystalline λ-type Bence-Jones dimer show that there is a binding site within this hydrophobic pocket for some hapten molecules (Edmundson et al., 1974). The amino acid residues, which form the binding cavity in this λ-type Bence-Jones dimer are almost identical and their spatial arrangement is very similar to that of the V_{REI} dimer. It is important, however, that the Gln-89 residues present in the V_{REI} dimer, where they form the bottom of the hapten binding pocket, are exchanged by the much smaller Ser residues (Ser-91) in the λ-type Bence-Jones dimer, perhaps making the cavity more accessible for haptens than in REI. At the bottom of the hapten binding cavity of REI, another solvent molecule is localized near the polar groups of the side chains of the two Asn-34 residues.

Structural Reasons for Conserved Amino Acid Residues. A comparison of amino acid sequences of variable portions of light chains (Dayhoff, 1972) shows a number of invariant or almost completely conserved amino acid residues both in κ and λ chains. The functions of Cys-23, Cys-88, and Trp-35 have been discussed before. Gln-6 conserved in all light chains is internal, its side chain hydrogen bonded to Tyr-86 C=O and Thr-102 OH (for distances see Table III); Gly-16, Gly-41, and Gly-57 are involved in hairpin bends of type II (Table IV), in which the third residue must be Gly; Gly-99 and Gly-101 are invariant in all light chains. An inspection of the model shows that no larger amino acid residues fit at those positions, as C$^\beta$ of an exchanged Gly-99 residue would interfere with the side chain of Gln-6 and the C$^\beta$ of an exchanged Gly-101 residue would interfere with the side chain of Tyr-87. The invariant amino acids Arg-61 and Asp-82 form a salt link and are hydrogen-bonded to each other. Tyr-86 is internal, its phenol-OH being hydrogen-bonded to Asp-82 C=O. Phe-98, also invariant in all light chains, is strongly involved in the dimer contact region, as are some other almost completely conserved residues (Tyr-36, Gln-38, Pro-44, and Tyr-87). Proline-8 and Pro-95 are nearly invariant in κ chains; these are *cis*-prolines, they occur in the third positions of reverse turns as mentioned above.

Hapten Binding Studies. V_{REI} dimer can be considered as a primitive antibody (Epp et al., 1974). Binding experiments with Dnp (2,4-dinitrophenyl) derivatives as hapten molecules have been made. An aromatic ring with polar substituents might be a suitable hapten, because of the participating amino acid residues in the hapten binding site (mainly tyrosines and two asparagines, see Figure 6) and their spatial arrangement. For some compounds (di-Dnp-Tyr-Gly, di-Dnp-3-I-Tyr, Dnp-di(-*O*-Dnp-Tyr)) preliminary equilibrium dialysis measurements gave binding constants of about 10^2–10^4 l./mol. The Dnp-di(-*O*-Dnp-Tyr) compound was synthesized because it has twofold symmetry like the V_{REI} dimer. It also showed the highest binding constant. These compounds appear to bind also to crystals of the V_{REI} protein. Crystallographic studies are in progress.

Four molecular structures of components of myeloma proteins and Bence-Jones proteins were reported at high resolution (Segal et al., 1974; Poljak et al., 1974; Schiffer et al., 1973; Epp et al., 1974) and also binding studies of possible hapten molecules were performed (Padlan et al., 1974; Amzel et al., 1974; Edmundson et al., 1974). The present work was done to get an accurate molecular model of the V_{REI} dimer, which may be regarded as a primitive antibody equivalent, although consisting only of two identical variable portions of a Bence-Jones protein. The quality of the crystals allowed a constrained crystallographic refinement at a resolution of 2.0 Å, which yields a final molecular model with atomic positions accurate to about 0.2 Å. The precise knowledge of the V_{REI} dimer enabled a crystal structure analysis of a related molecule by Patterson search

Table VI: Distances of Solvent Molecules to Polar Groups of the Dimer, Calculated between 2.2 and 3.3 Å.[a]

Atom	d (Å)	Solvent Molecule	d (Å)	Atom
Met-4 N	3.3	404	2.8	Phe-98 C=O
Trp-35 NE1	2.7	406	3.0	Ala-51 C=O
Ser-10 OG	3.1	431	3.0	Ser-12 OG
Ile-2 N	2.8	435	3.2	Pro-95 C=O
Thr-5 C=O	3.2	436	3.0	Thr-22 OG1
Glu-81 C=O	3.0	438	3.1	Asp-82 OD2
Tyr-49 OEE	3.1	440	3.0	Tyr-91 OEE
Tyr-87 OEE	2.6	449	3.1	Gln-100 C=O
Ser-293 C=O	3.0	405	2.4	Pro-295 C=O
Ser-277 OG	2.9	412	2.9	Gln-279 NOE2
Gln-238 C=O	3.1	416	3.3	Thr-285 OG1
Trp-235 NE1	2.7	420	2.9	Ala-251 C=O
Tyr-296 OEE	2.6	443	3.2	Tyr-291 C=O
Thr-239 N	2.8	444	2.6	Ala-243 C=O
Glu-281 C=O	2.6	450	2.8	Asp-282 OD1
Tyr-96 C=O	2.6	429	2.9	Leu-246 N
Thr-5 OG1	3.2	402		
Ile-83 C=O	2.6	407	3.2	441 H_2O
Thr-85 OG1	3.3	408	2.5	425 H_2O
Thr-91 C=O	3.3	413		
Asp-17 OD2	2.9	418		
Leu-104 C=O	3.2	425		
Phe-62 C=O	3.0	433		
Leu-54 C=O	2.3	434		
Gln-79 NOE2	2.3	439		
Glu-50 C=O	3.2	442		
Val-58 C=O	3.0	447		
Asp-17 OD1	3.1	451		
Met-204 N	2.7	403		
Leu-304 C=O	3.2	409		
Asp-217 OD2	3.1	414		
Ser-277 OG	3.2	426		
Phe-262 C=O	3.1	445		
Gln-237 NOE2	3.2	448		
Ser-252 OG	3.1	452		
Ser-252 C=O	2.5	453		

[a] Subunit 2 of the dimer has 200 added to amino acid numbers, solvent molecules have 400 to their optional numbers.

techniques (Fehlhammer et al., 1975). It should be further possible to study more precisely the binding of hapten molecules and the subtle structural changes which might occur, using difference Fourier maps because refined phases are considerably better than isomorphous phases (Deisenhofer and Steigemann, 1975; Huber et al., 1974; Watenpaugh et al., 1973).

Acknowledgments

We thank Drs. H. Deisenhofer and W. Steigemann for helpful discussions and the use of their programs. B. Theile did most of the X-ray photographic work, and U. Kohl most of the chemical work. M. Sauer helped us with the calculations, E. Preuss and K. Epp with the drawings. All calculations were made at the Rechenzentrum des Max-Planck-Institutes für Biochemie. The help of the staff was of great value.

References

Amzel, L. M., Poljak, R. J., Saul, F., Varga, J. M., and Richards, F. F. (1974), *Proc. Natl. Acad. Sci. U.S.A. 71,* 1427.

Arnott, S., Dover, S. D., and Elliott, A. (1967), *J. Mol. Biol. 30,* 201.

Beychok, S. (1967), in Biological Macromolecules Series, Vol. 1, Poly-α-Amino Acids, Fasman, G. D., Ed., New York, N.Y., Marcel Dekker, p 315.

Crawford, J. L., Lipscomb, W. N., and Schellmann, C. G. (1973), *Proc. Natl. Acad. Sci. U.S.A. 70,* 538.

Cruickshank, D. W. J. (1949), *Acta Crystallogr. 2,* 65.

Dayhoff, M. O., Ed. (1972), Atlas of Protein Sequence and Structure, Vol. V, Silver Spring, Md., National Biomedical Research Foundation, p D-256.

Deisenhofer, J., and Steigemann, W. (1975), *Acta Crystallogr., Sect. B 31,* 238.

Diamond, R. (1966), *Acta Crystallogr., Sect. A 21,* 253.

Diamond, R. (1971), *Acta Crystallogr., Sect. A 27,* 436.

Diamond, R. (1974), *J. Mol. Biol. 82,* 371.

Edmundson, A. B., Ely, K. R., Girling, R. L., Abola, E. E., Schiffer, M., Westholm, F. A., Fausch, M. D., and Deutsch, H. E. (1974), *Biochemistry 13,* 3816.

Epp, O., Colman, P., Fehlhammer, H., Bode, W., Schiffer, M., Huber, R., and Palm, W. (1974), *Eur. J. Biochem. 45,* 513.

Fehlhammer, H., Schiffer, M., Epp, O., Colman, P. M., Lattman, E. E., Schwager, P., and Steigemann, W. (1975), *Biophys. Struct. Mech. 1,* 139.

Forsyth, J. B., and Wells, M. (1959), *Acta Crystallogr. 12,* 412.

Huber, R., and Kopfmann, G. (1969), *Acta Crystallogr., Sect. A 25,* 143.

Huber, R., Kukla, D., Bode, W., Schwager, P., Bartels, K., Deisenhofer, J., and Steigemann, W. (1974), *J. Mol. Biol. 89,* 73.

Huber, R., and Steigemann, W. (1974), *FEBS Lett. 48,* 235.

IUPAC–IUB Commission on Biochemical Nomenclature (1970), *Biochemistry 9,* 3471.

Padlan, E. A., Segal, D. M., Cohen, G. H., Davies, D. R., Rudikoff, S., and Potter, M. (1974), in The Immune System, Sercarz, E. E., Williamson, A. R., and Cox, C. F., Ed., New York, N.Y., Academic Press, p 7.

Palm, W. H. (1970), *FEBS Lett. 10,* 46.

Palm, W. (1974), *Hoppe-Seyler's Z. Physiol. Chem. 355,* 872.

Palm, W. H., and Hilschmann, N. (1973), *Hoppe-Seyler's Z. Physiol. Chem. 354,* 1651.

Palm, W., and Hilschmann, N. (1975), *Hoppe-Seyler's Z. Physiol. Chem. 356,* 167.

Poljak, R. J., Amzel, L. M., Chen, B. L., Phizackerley, R. P., and Saul, F. (1974), *Proc. Natl. Acad. Sci. U.S.A. 71,* 3440.

Schiffer, M., Girling, R. L., Ely, K. R., and Edmundson, A. B. (1973), *Biochemistry 12,* 4620.

Schwager, P., Bartels, K., and Jones, A. (1975), *J. Appl. Crystallogr. 8,* 275.

Segal, D. M., Padlan, E. A., Cohen, G. H., Rudikoff, S., Potter, M., and Davies, D. R. (1974), *Proc. Natl. Acad. Sci. U.S.A. 71,* 4298.

Steigemann, W. (1974), Ph.D. Thesis, Technische Universität, München.

Stout, G. H., and Jensen, L. H. (1968), in X-Ray Structure Determination, New York, N.Y., Macmillan.

Venkatachalam, C. M. (1968), *Biopolymers 6,* 1425.

Watenpaugh, K. D., Sieker, L. C., Herriott, J. R., and Jensen, L. H. (1973), *Acta Crystallogr., Sect. B 29,* 943.